Published in final edited form as:
Supramol Chem. 2010 November ; 22(11-12): 862–869. doi:10.1080/10610278.2010.510263.

Self-assembled cation transporters made from lipophilic 8-phenyl-2'-deoxyguanosine derivatives

Mariana Martín-Hidalgo, **Karla Camacho-Soto**, **Vladimir Gubala**, and **José M. Rivera***
Department of Chemistry, University of Puerto Rico, Río Piedras Campus, Río Piedras, Puerto Rico 00931

Abstract

We have previously reported that 8-phenyl-2'-deoxyguanosine derivatives (8PhGs) are able to extract metal cations from an aqueous phase into an organic phase. Herein we report on the ability of 8PhGs to transport metal cations across a bulk lipophilic liquid membrane. The experiments were performed using lithium, sodium, potassium, and strontium picrate salts with the parent lipophilic **Gi**, two isomeric 8PhG derivatives, *cis*-dicyclohexano-18-crown-6 (**CD18C6**) and **[2• 2• 2]**cryptand as reference compounds. The relative amounts of the picrate salts were measured by UV spectroscopy in both, the source phase and the receiving phase over a period of 24 h. The results show that the transport efficiency of the self-assembled ionophores formed by 8PhGs is either similar or superior to that of **CD18C6**, and in all but one case higher than the parent compound **Gi**. The varying efficiencies between the derivatives can be attributed to the stability (kinetic and thermodynamic) and the different molecularities of the supramolecules formed by these 8PhGs. The ease of the synthesis of 8PhGs, their anion independent assembly and the fact that the transport efficiency can be modulated as a function of the structure of the 8PhGs bode well for the use of such compounds in the development of novel antimicrobial agents and cation sensing devices.

Keywords

self-assembly; ion transport; cation recognition

Introduction

Cation recognition has played a prominent role in supramolecular chemistry ever since the early days of the field.[1–4] Cation recognition evolved towards the development of functional systems such as carriers and channels, which were able to transport ions across lipophilic membranes. The use of bulk liquid membrane systems,[5] have provided a simple resource to mimic the ion transport properties of the natural polyether antibiotic ionophores.[6, 7] The characterization of the resulting host–guest complexes, make possible the determination of the principles behind the dynamic equilibrium at the aqueous/organic interface.[8, 9] Furthermore, these synthetic carriers have found uses in the development of sensors, drug delivery, as well as in environmental separations and waste remediation.[4] These derivatives are characterized by having preorganized conformations constrained by covalent bonds and high affinities, which in turn can limit their ion transport efficiency due to slow decomplexation kinetics. Alternatively, self-assembly allows the construction of supramolecular ionophores that are not only easier to make, but also enables a proper

*Corresponding author. jmrivortz@mac.com.

balance between ion affinity and ion exchange kinetics. This in turn facilitates the optimization of the transport properties via a fine-tuning of noncovalent interactions (e.g., hydrogen bonds, π-π interactions, van der Waals forces).

The groups of Gotarelli, Spada and Davis have pioneered the construction of self-assembled ionophores (SAIs) based on sugar-modified lipophilic guanosine (G) and iso-guanosine (iG) derivatives.[10, 11] Self-assembled planar guanosine tetramers are known to stack in the presence of a wide variety of cations (e.g., alkaline, alkaline earth), into supramolecules known as G-quadruplexes (GQs, Figure1). Such supramolecules are efficient at the extraction of alkali and alkaline earth picrate salts from an aqueous phase into an organic phase. For example, Reinhoudt and Davis *et al.* reported high selectivity and efficiency in the extraction and transport of radioactive metal cations such as $^{137}Cs^{+}$ and $^{226}Ra^{2+}$ by a related self-assembled decamer formed by iG.[12] Furthermore, Davis has reported that for G-based SAIs the anion can play an active role modulating the dynamics of the resulting complexes when they are integral components of the supramolecule.[13]

We have reported the synthesis of a variety of 8-phenyl-2'-deoxyguanosine derivatives (8PhGs) and have shown that the supramolecular properties can be tuned by their structural, or intrinsic parameters.14 Specifically, the thermodynamic stability, molecularity and fidelity of such supramolecules is influenced by parameters such as: (a) the nature and the position of the functional group at the 8-phenyl ring,[14, 15] and (b) the nature and the size of the moieties attached to the 3'- and 5'-OH groups of the furanose ring.[16,17] The medium, or extrinsic parameters, also influences the assembly process.[18,19] For example, in organic media, and under identical conditions, the *meta*-acetylphenyl derivative (**mAGi**) assembles into a hexadecamer, while its *para*acetylphenyl isomer (**pAGi**) assembles into an octamer (Figure 1).[14]

We have also reported that such base-modified 8PhGs are effective SAIs that enable the extraction of cations from an aqueous phase into an organic phase.[20] Their extracting ability was also modulated by the presence and substitution pattern of the 8-phenyl ring. We have not yet reported, however, the corresponding transport properties of such derivatives. Herein we report that within the context of a bulk membrane model system, selected 8PhGs are also effective carriers of various cation picrate salts against a concentration gradient via a symport mechanism.[21, 22]

Results

Two isomeric 8PhG derivatives (**pAGi**, **mAGi**) and the parent compound **Gi** (Figure 2a) were evaluated for their ability to transport the picrate salts of potassium, sodium, lithium, and strontium. In parallel, two well known covalent ionophores, *cis*-dicyclohexyl-18-crown-6 (**DC18C6**) and the **[2.2.2]** cryptand[23] (Figure 2b, 0.625 mM solution of ionophore in $CHCl_3$), were also evaluated to calibrate the transport properties of the 8PhG derivatives.

We used a Schulman bridge experimental set up and monitored the cation transport indirectly by measuring the corresponding picrate counter anions via UV/Vis spectroscopy (Figure 3). We present the data in four graphs (one per cation) of percentage transported out of the source phase (*S*, 20 mM MPic aqueous solution) and into the receiving phase (*R*, nanopure water) over a period of 24 h.[5,8] We also, show tabulated data corresponding to each one of the graphs containing the corresponding values at 1, 5, 10, and 24 h. This provides four snapshots of the transport process in an explicit and quantitative manner. The tables also provide the data corresponding to the amount of cation that remains partitioned within the membrane (*M*) at each corresponding time.

Furthermore, the tables include two parameters, the efficiency factor (E_F) and the overall efficiency (O_E), that should also facilitate the analysis and discussion of the data. A transporter that acts as a cation carrier must bind to it at the source-membrane interphase and release it at the membrane-receiving interphase. This is in contrast with a cation channel, where the cation passes through a hole provided by the transporter. Thus, as it has been previously shown, the optimal transport is obtained with an intermediate cation affinity, not too low (otherwise no cation will be complexed into the membrane), but not too high either (because the cation will get stuck complexed within the membrane).[8] An ideal carrier efficiently moves the cation from one interphase to the other, keeping a minimal amount of cation within the membrane during the process and no cation at all once the gradient that drives the transport is dissipated. The E_F provides a way to compare the efficiency of transport taking in consideration not only how much cation makes it to the receiving phase, but also how much remains within the membrane. The efficiency factor ($E_F = R/(R+M)$) represents how much of the cation that left the source phase made it to the receiving phase. The closer this number is to unity the better. The overall efficiency ($O_E = E_F*R$), then, provides a convenient parameter to directly compare how effective is a given transporter at a particular time. For the purposes of the discussion we will focus the discussion on the overall efficiency after 24 h, highlighting other parameters whenever appropriate.

Transport of Potassium Picrate

For potassium picrate, after 24 h, the overall efficiency decreases in the following order: **pAGi** > **DC18C6** ~ **mAGi** > **Gi** ~ **2.2.2** (Figure 4). **pAGi** is the most effective transporter with an O_E that is twice as large as that of **DC18C6** and **mAGi** (Table 1). The parent compound **Gi** is a significantly weaker transporter when compared to **mAGi** and **pAGi** as reflected in its low E_F and O_E values. The amount of potassium cation that **Gi, DC18C6**, and **2.2.2** load up into the membrane after 1 h remains effectively unchanged after 24 h. On the other hand, while both **mAGi** and **pAGi**, load up about 20% potassium after 1 h, after 24 h the amounts remaining in the membrane decrease to 13% and 2%, respectively. In essence, **pAGi** is the best transporter for potassium, not just because it transports the greatest proportion of potassium to the receiving phase, but also because it keeps the least amount of it within the membrane as reflected in the corresponding large E_F and O_E values. **2.2.2** is the least efficient transporter of all, as expected for an ionophore with a high binding affinity due to low decomplexation kinetics.[8]

Transport of Sodium Picrate

For sodium picrate, after 24 h, the overall efficiency is relatively high to moderate for all the compounds studied and decreases in the following order: **mAGi** ~ **pAGi** ~ **DC18C6** > **Gi** (Figure 5). In general, sodium was transported more effectively by all of the tested ionophores than any other cation studied. In particular, **mAGi**, **pAGi** and **DC18C6** show similarly large E_F and O_E values for sodium (Table 2). The parent compound **Gi**, although the least efficient transporter for this cation, still shows the best performance when compared to its efficiency with the other cations studied. Parallel to the results with potassium, the efficiency of transport of sodium, for all the ionophores tested, is excellent not only because of the high total amount transported, but also because in most cases the amount of sodium that remained in the membrane (after 24 h) was similarly low. Specifically, **DC18C6** and **mAGi** kept the lowest amounts of sodium (7% and 5%); although after 1 h **Gi** and **pAGi** loaded relatively large amounts of sodium in the membrane (24% and 28%), after 24 h those values settled down to below 10% (Table 2).

Transport of Lithium Picrate

For lithium picrate, after 24 h, the overall efficiency is generally low for all the compounds studied and decreases in the following order: **Gi** > **DC18C6** ~ **mAGi** ~ **pAGi** (Figure 6).

The parent **Gi**, after 24 h, is the most effective transporter with an O_E that is at least twice as large as those of the other ionophores (Table 3). Due to the large proportion of lithium that remained within the membrane, however, the corresponding E_F value for **Gi** is 0.6. In fact, the poor transport properties for lithium were exacerbated by a tendency for this cation to be accumulated within the membrane. The control compound **DC18C6**, which is known to have a low affinity for lithium,[23] showed a low efficiency in both extraction and transport similar to those observed for **mAGi** and **pAGi**. The latter fared worst of all accumulating twice as much lithium in the membrane than the amount that made it to the receiving phase (E_F = 0.3). This behavior is consistent with our previous report that showed **pAGi** to be good extracting lithium picrate into an organic phase.[20]

Transport of Strontium Picrate

For strontium picrate, after 24 h, the overall efficiency decreases in the following order: **pAGi** > **mAGi** > **DC18C6** ~ **Gi** (Figure 7). **pAGi**, after 24 h, is the most effective transporter with the highest O_E value, while for **mAGi** the corresponding value is lower not only because it transported slightly less strontium (Table 4), but also because it kept almost twice as much of this cation in the membrane. The parent **Gi** and **DC18C6** showed similarly poor transport properties (O_E < 10%),[24] reaching a steady state within 2.5 h of with an average *R* value of 15%. Although the transport of strontium was generally more effective than that of lithium, it also suffered from a tendency to be accumulated within the membrane as reflected by similarly low E_F values (Table 4).

The kinetics of transport for lithium and strontium deviate from that observed for potassium and sodium as evidenced by the overall shapes of the transport curves (Figure 4–7). With lithium, **DC18C6** reaches a steady state within the first hour (*R* ~ 10%), whereas with **mAGi** and **pAGi** it takes around ten hours to reach a similar steady state. Conversely, after 10 h the *R* value for **Gi** had already surpassed 10% reaching twice that amount over 24 h, although at this time it still had not reached a steady state (i.e., the rate of transport still has a positive slope). With strontium, **mAGi** and **pAGi** show transport curves that are similar to those with potassium and sodium but **Gi** and **DC18C6**, as mentioned previously, reached a transport steady state within 2.5 h.

Discussion

The differences in the efficiency of transport, across a lipophilic membrane, for a cation are dictated by factors such as the affinity of the cation for a given ionophore, the free energies of hydration/dehydration, the nature of the counteranion, and the lipophilicity of the ionophore. For SAIs the dynamics of cation transport and that of the assembling subunits influence one another to make the resulting transport more or less efficient. In the case of 8PhGs, the molecularity of the resulting assemblies is also likely to play an important role in such transport.

For example, the high efficiency of transport for potassium by **pAGi** can be explained by the increased binding capacity of the resulting assembly, when compared to its isomeric congener **mAGi**. Molecular modeling studies suggest that the acetyl groups in the *para* position of the **pAGi** subunits could come into close proximity with the 5'-isobutyric ester groups and form additional binding pockets on the surface of the assembly.[20] Conversely, the lower transport efficiency for the same cation exhibited by **mAGi** is likely due to the increased stability of the resulting supramolecule. **mAGi** has a strong propensity to form a hexadecamer with good fidelity, which we have shown to be thermodynamically more stable than the octamer formed by **pAGi**.[14] The hexadecamer consists of four G-tetrads stacked upon each other forming a central channel occupied by three potassium cations (Figure 1a). The reported high selectivity shown by guanine analogues for the potassium cations (1.38

Å)[25] over the other monovalent cations studied,[13, 26, 27] makes it suitable for the templation of highly stable GQs.

Sodium has been shown to be a good templating metal cation (1.02 Å)[25] for the formation of GQs.27 The preferential hydration of sodium over potassium cations, can also explain the efficiency in the release of the former by **mAGi** and **pAGi**. This has also been suggested as an explanation for the reported selectivity of potassium over sodium cations in the templation of related G-quadruplex DNA structures.[28]

It is has been reported extensively that a small cation like lithium does not effectively template the formation of stable GQs.[29, 30] Since an efficient transport process requires the formation of a minimally stable complex between the cation and the ionophore, it is not surprising then that the assemblies formed by **mAGi** and **pAGi** show a low transport efficiency for lithium cations (0.76 Å).[25] The energetically costly ($\Delta G_{hydration} = -475$ kJ/mol)[23] transfer of lithium from aqueous source phase into a lipophilic membrane, likely plays a role in the poor efficiency of transport.

When compared to **pAGi**, **mAGi** showed a diminished transport efficiency with both potassium and strontium cations. Although both cations have similar ionic radii (1.38 Å, 1.26 Å respectively),[25] this can be rationalized by the putative higher affinity of the SAIs formed by strontium (similar to what has been shown by related quadruplexes),31 as evidenced by the relatively high amounts of such cations it kept within the membrane after 24 h (Tables 1, 4).

The generally poor transport efficiency shown by **Gi** with all the metal cations tested can be attributed to the fact that this is the only derivative, in which both the metal ion and picrate anion could be integrated components of the assembly. The picrate anions are expected to actively influence the assembly's stability and dynamics, in a manner similar to that reported by the Davis group with related lipophilic guanosine derivatives.[13] In contrast, 8PhGs are expected to show a relatively anion-independent assembly due to the steric blocking by the C8-phenyl groups, which should prevent the picrate anions from playing an active role in the resulting assembly, thus minimally affecting their transport efficiency.

Why, for a given cation, do some transporters show a relatively large initial loading of salt within the membrane, which in some cases decrease up to an order of magnitude after 24 h (e.g., **pAGi** with potassium)? A large gradient obliges more salt to go into the membrane, but when the gradient dissipates the amount of salt that remains loaded within the membrane decreases to a minimal baseline value. Early in the experiment, when the gradient is larger, it is energetically favorable for the system to load up a maximal amount of salt. Such amount is determined by factors like the salt's desolvation energy, the ionophore's concentration within the membrane as well as its ion binding affinity, which in turn depends on the kinetics of ion binding to (k_{on}) and releasing from (k_{off}) the ionophore (Figure 3). In contrast to the aforementioned factors that remain constant throughout the experiment, the magnitude of the gradient decreases towards zero as the time evolves. As the concentration of salt in the source phase becomes more similar to that of the receiving phase the amount of salt that remains loaded within the membrane decreases to a minimal equilibrium baseline value.

Conclusion

We showed that attaching a substituted phenyl ring to the C8 of a guanine base leads to SAIs with enhanced transport properties, when compared to the unsubstituted parent compound. Furthermore, these SAIs proved to be equal or better transporters for potassium, sodium and strontium than the well-known **DC18C6** ionophore. The structural modification at the C8 of

the guanine base serves to modulate the discrimination of these derivatives for specific cations. For example, the superior transport efficiency for potassium cations shown by **pAGi** relative to **mAGi** can be attributed to the putative surface binding sites on the assembly of the former combined with the enhanced stability of the assembly of the latter. Conversely, after 24 h the best transporter for lithium was the parent **Gi**, not because of an overall enhanced transport efficiency, but because of the comparatively poor transport efficiency shown by the 8PhGs and **DC18C6**. Moreover, the fact that the SAIs made from 8PhGs do not require picrate anions for their formation may facilitate their incorporation into liposomal membranes and may enable the formation of artificial self-assembled transmembrane ion channels.[32] Whether or not these or related 8PhGs can be incorporated into the lipid membranes of vesicles and if they will self-assemble in such environments is still to be determined. If they do, it will be interesting to determine if they retain their transport activity acting as carriers or via the formation of ion channels. These and other questions will remain open until a future report.

Experimental

Transport experiments

A solution of the crystalline guanosine derivative (prepared as described previously15) in distilled and dried $CHCl_3$ (6 mL, 5 mM of a monomer = 0.625 mM of a theoretical octamer) or **DC18C6** (6 mL, 0.625 mM), was placed in a 20 mL beaker (I.D. = 2.861 cm) equipped with magnetic stirring bar. A solution of aqueous picrate (6 mL, 20 mM) as a source phase and nanopure water (6 mL) as a receiving phase (inner tube I.D. = 1.526 cm, O.D. = 1.891 cm), were simultaneously added to their compartments. This mixture was stirred at 500 rpm and aliquots (10 μL) from both the source and receiving phase were concurrently taken every 5 minutes in the first 0.5 h, every 10 min in the second 0.5 h, every 15 minutes in the third 0.5 h and every 60 minutes for the next 22.5 h. Each sample was diluted with nanopure water (4 mL) and its absorbance at 355 nm was measured using a UV-Vis spectrometer (Cary 100).

The experiments were performed using a Schulman bridge apparatus, which is an adaptation of the "U-tube" apparatus developed in 1970 by Ashton and Steinrauf (Figure S1).[33] A picture of the apparatus is included in the supplementary information.

Data Analysis

The concentration of the metal picrate was monitored in both aqueous compartments as a function of time. The simultaneous recording of both phases enables the determination of accurate values for the relative speeds transport for different carriers and the mass balance of the system. The amount of metal picrate in both the source and the receiving phases was determined using a calibration curve applying the Beer-Lambert's law. All the measurements were performed in triplicate in order to ensure reproducibility and to obtain reliable results. The data was analyzed using Microsoft Excel 2007, version 11.2.5; dilution coefficient (400.8), volume coefficient (2 mL), normalization (normalized per 10 mmol of the derivative), standard deviation and charge of divalent alkaline earth metal cations were taken into consideration when calculating the final results. The final data sheets were exported and plotted using Origin 7.0. A version of Figures 4–7 showing the graphs with the corresponding error bars are included in the supplementary information.

Supplementary Material

Refer to Web version on PubMed Central for supplementary material.

Acknowledgments

We thank Doriann de Jesús and Rosa Haddock for technical support during the initial stages of this work and Marilyn García-Arriaga for the preparation of molecular models. MMH thanks NIH-RISE (2 R25 GM61151), Alfred P. Sloan Foundation and PRIDCO and KCS thanks NIH-MARC (5 T38 GM07821) for financial support.

References

1. Gokel GW, Carasel I. Chem. Soc. Rev 2007;36:378–389. [PubMed: 17264938]
2. Chen XM, Izatt RM, Oscarson JL. Chem. Rev 1994;94:467–517.
3. Izatt RM, Zhang XX, An HY, Zhu CY, Bradshaw JS. Inorg. Chem 1994;33:1007–1010.
4. Gokel GW, Leevy WM, Weber ME. Chem. Rev 2004;104:2723–2750. [PubMed: 15137805]
5. Visser HC, Reinhoudt DN, de Jong F. Chem. Soc. Rev 1994;23:75–81.
6. Lenh JM. Pure & Appl. Chem 1979;51:979–997.
7. Painter GR, Pressman BC. Top. Current. Chem 1982;101:83–110.
8. Behr JP, Kirch M, Lehn JM. J. Am. Chem. Soc 1985;107:241–246.
9. Fyles TM. Can. J. Chem 1987;65:884–891.
10. Davis JT, Spada GP. Chem. Soc. Rev 2007;36:296–313. [PubMed: 17264931]
11. Davis JT. Angew. Chem. Int. Ed 2004;43:668–698.
12. van Leeuwen FWB, Verboom W, Shi XD, Davis JT, Reinhoudt DN. J. Am. Chem. Soc 2004;126:16575–16581. [PubMed: 15600363]
13. Shi XD, Mullaugh KM, Fettinger JC, Jiang Y, Hofstadler SA, Davis JT. J. Am. Chem. Soc 2003;125:10830–10841. [PubMed: 12952462]
14. Gubala V, Betancourt JE, Rivera JM. Org. Lett 2004;6:4735–4738. [PubMed: 15575673]
15. Rivera-Sanchéz, MdC; García-Arriaga, M.; Andújar-de-Sanctis, I.; Gubala, V.; Hobley, G.; Rivera, JM. J. Am. Chem. Soc 2009;131:10403–10405. [PubMed: 19722619]
16. Betancourt JE, Rivera JM. Org. Lett 2008;10:2287–2290. [PubMed: 18452304]
17. García-Arriaga M, Hobley G, Rivera JM. J. Am. Chem. Soc 2008;130:10492–10493. [PubMed: 18642917]
18. Betancourt JE, Martín-Hidalgo M, Gubala V, Rivera JM. J. Am. Chem. Soc 2009;131:3186–3188. [PubMed: 19216522]
19. Betancourt JE, Rivera JM. J. Am. Chem. Soc 2009;131:16666–16668. [PubMed: 19883053]
20. Gubala V, De Jesús D, Rivera JM. Tetrahedron Lett 2006;47:1413–1416.
21. Behr JP, Lehn JM. J. Am. Chem. Soc 1973;95:6108–6110. [PubMed: 4733834]
22. Kobuke Y, Hanji K, Horiguchi K, Asada M, Nakayama Y, Furukawa J. J. Am. Chem. Soc 1976;98:7414–7419.
23. Steed, JW.; Atwood, JL. Supramolecular Chemistry. Chichester: John Wiley & Sons, LTD; 2000.
24. Lamb J, Christensen J, Oscarson J, Nielsen B, Asay B, Izatt R. J. Am. Chem. Soc 1980;102:6820–6824. The binding constant between the host-guest complex between strontium ions and DC18C6 were reported in methanol solution.
25. Shannon RD. Acta Crystallogr., Sect. A 1976;32:751–767.
26. Wlodarczyk A, Grzybowski P, Patkowski A, Dobek A. J. Phys. Chem. B 2005;109:3594–3605. [PubMed: 16851398]
27. Neidle, S.; Balasubramanian, S. Quadruplex Nucleic Acids, The Royal Society of Chemistry. Cambridge: 2006.
28. Hud NV, Smith FW, Anet FA, Feigon J. Biochemistry 1996;35:15383–15390. [PubMed: 8952490]
29. Wong A, Wu G. J. Am. Chem. Soc 2003;125:13895–13905. [PubMed: 14599230]
30. Davis JT, Tirumula S, Jenssen JR, Radler E, Fabris D. J. Org. Chem 1995;60:4167–4176.
31. Chen FM. Biochemistry 1992;31:3769–3776. [PubMed: 1567831]
32. Kaucher MS, Harrell WA, Davis JT. J. Am. Chem. Soc 2006;128:38–39. [PubMed: 16390110]
33. Ashton R, Steinrauf LK. J. Mol. Biol 1970;49:547–556. [PubMed: 5453345]

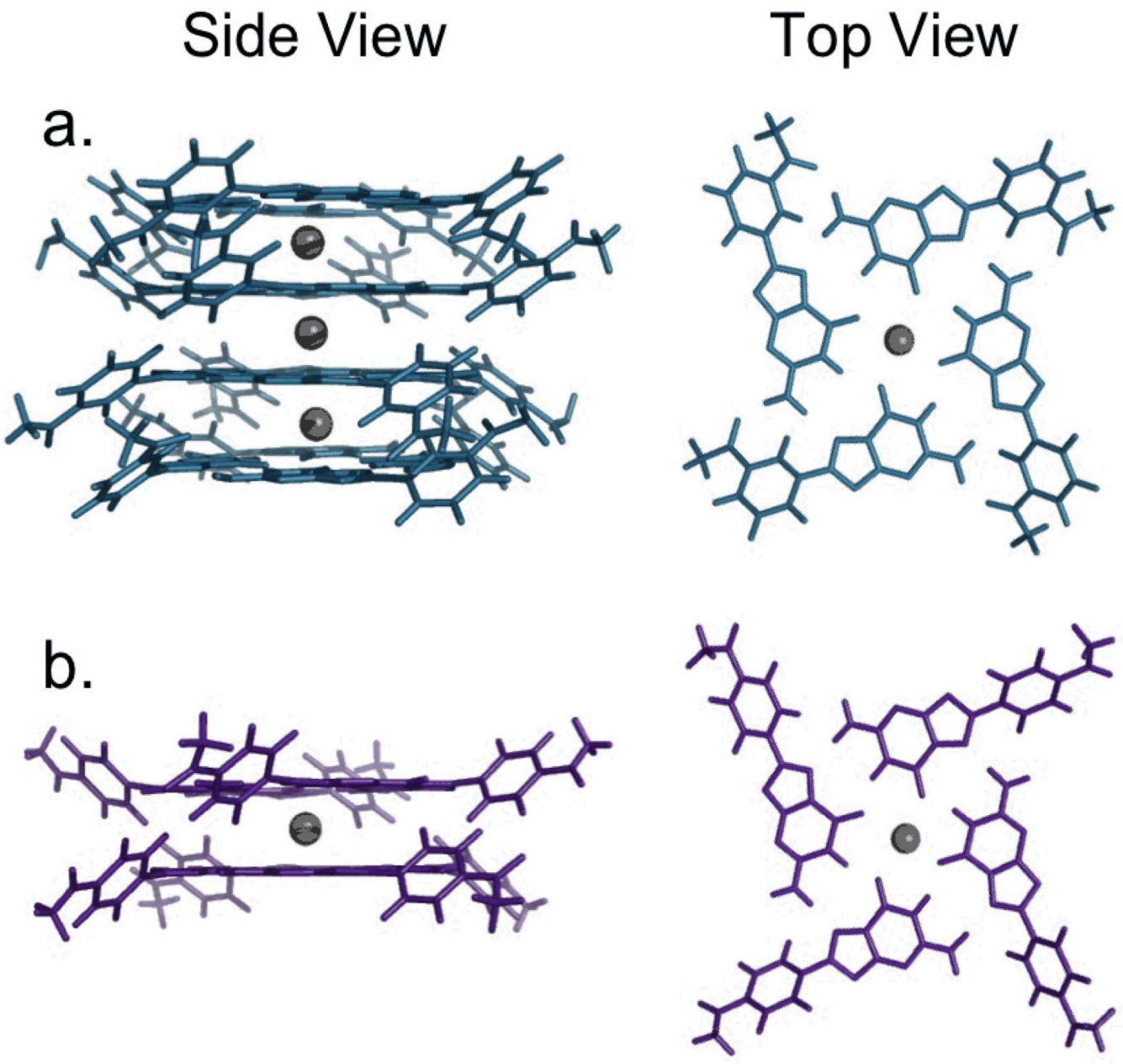

Figure 1.
Side (left) and top (right) views for molecular models of (a) (**mAGi**)$_{16}$• 3K$^+$ and (b) (**pAGi**)$_8$• K$^+$ GQs. The 2'-deoxyribose moiety and the lipophilic groups attached to it are not shown for clarity.

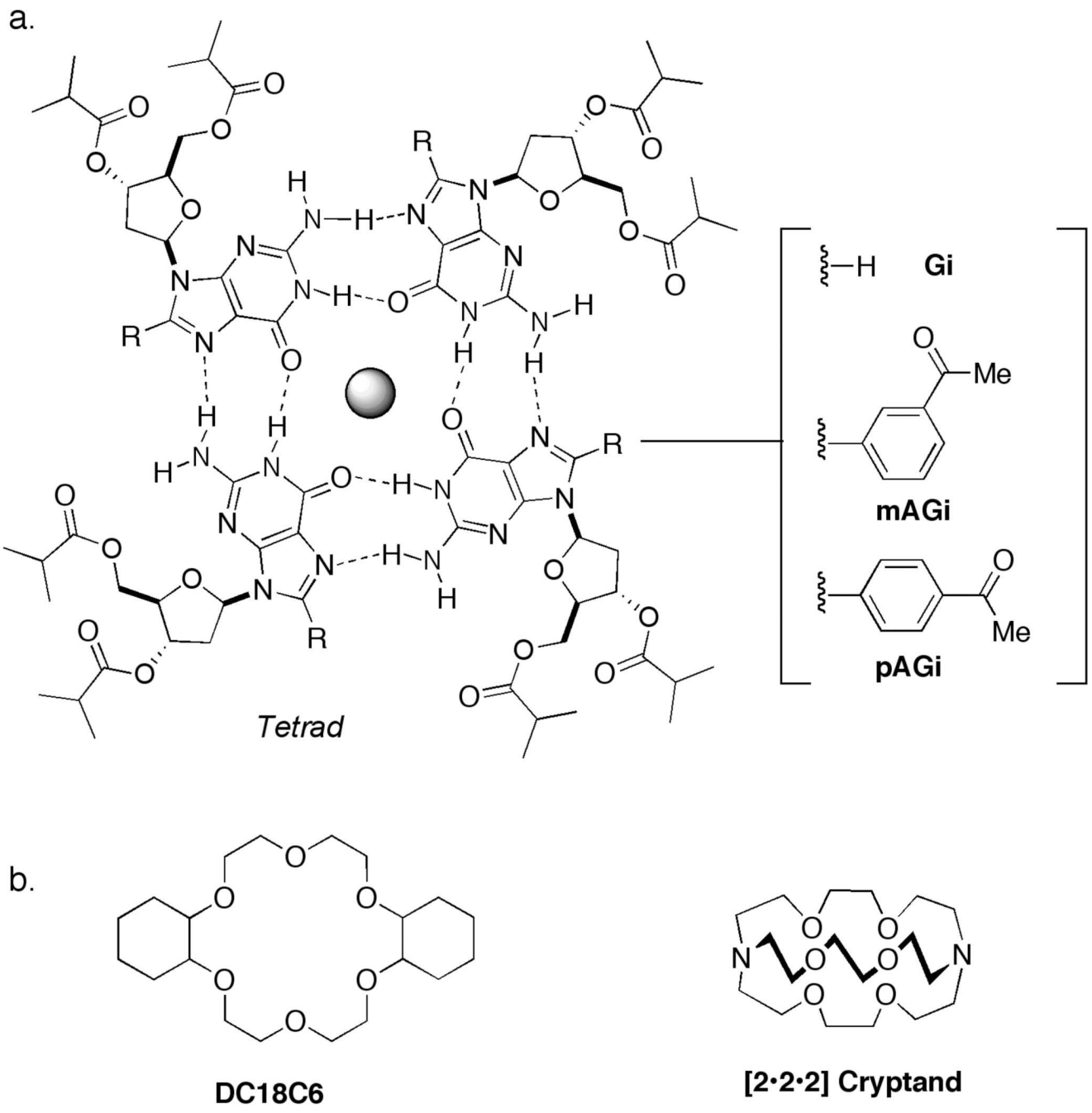

Figure 2.
(a) Tetrad formed by the various 2'-deoxyguanosine derivatives shown and (b) covalent ionophores used as reference compounds.

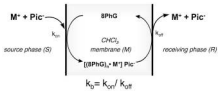

Figure 3.

Representation of a symport gradient pumping mechanism. M^+ = metal and Pic^- = picrate. K_b = binding constant, K_{on} = association constant, K_{off} = disassociation constant. (Adapted from reference 21)

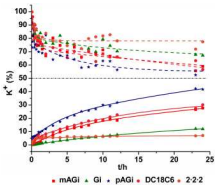

Figure 4.

Extraction and transport efficiency (mol %) of potassium picrate by 8PhGs, **DC18C6**, and **2.2.2** for a period of 24 h at 303 K. In this and Figures 5–7, values over 50% correspond to ions moving from the source phase to the bulk membrane and those below 50% represent ions moving from the bulk membrane into the receiving phase.

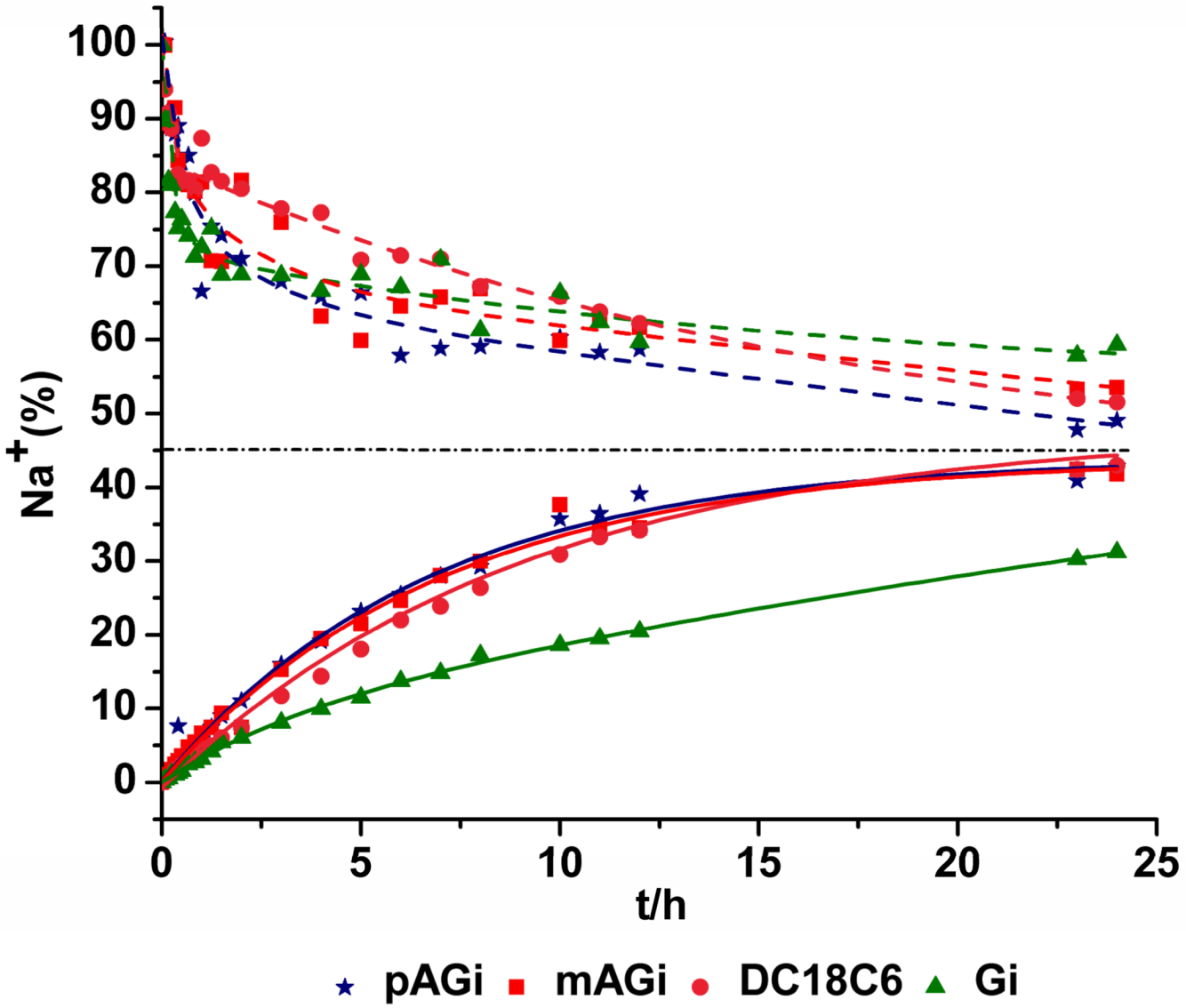

Figure 5.
Extraction and transport efficiency (mol %) of sodium picrate by 8PhGs and **DC18C6** for a period of 24 h at 303 K.

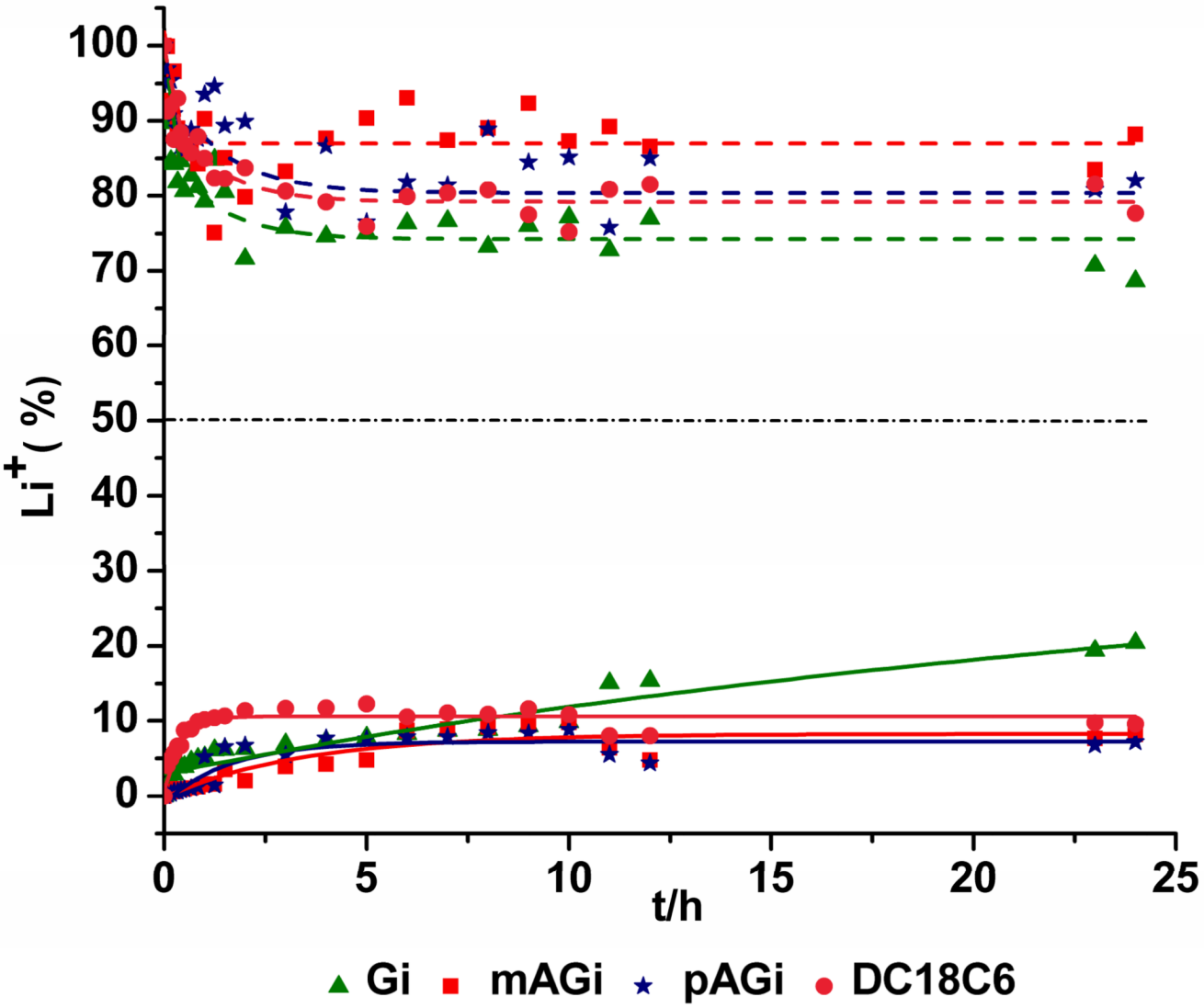

Figure 6.
Extraction and transport efficiency (mol %) of lithium picrate by 8PhGs and **DC18C6** for a period of 24 h at 303 K.

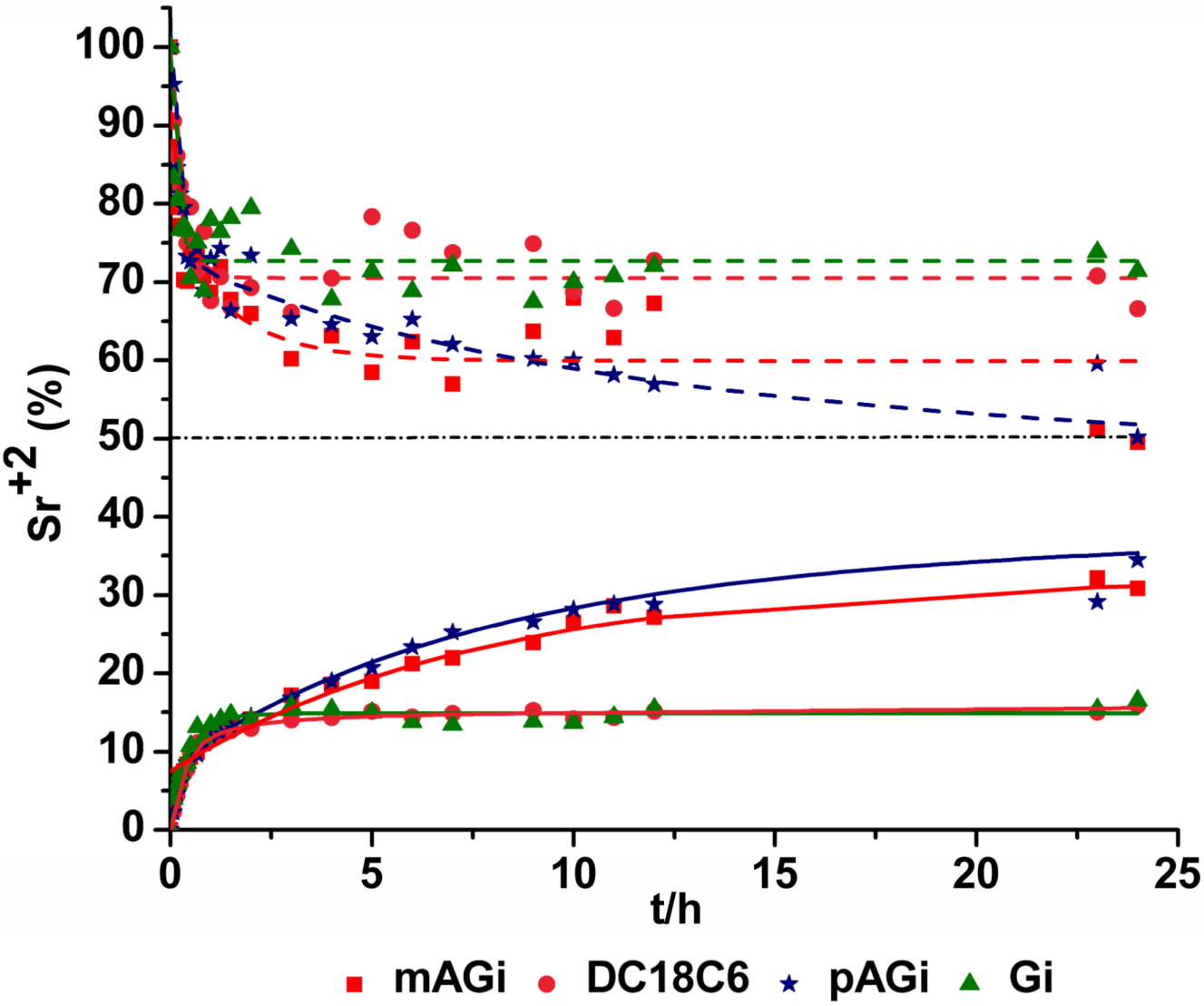

Figure 7.
Extraction and transport efficiency (mol %) of strontium picrate by 8PhGs and **DC18C6** for a period of 24 h at 303 K.

Table 1

Mol percentages of potassium cations in the source (*S*), membrane (*M*) and receiving (*R*) phases at selected times during a period of 24 h at 303 K.[(a)] The efficiency factor (E_F) and overall efficiency (O_E) were calculated as described in the text.

t/h	Gi					mAGi					pAGi					DC18C6					2.2.2				
	S	***M***	***R***	E_F	O_E	***S***	***M***	***R***	E_F	O_E	***S***	***M***	***R***	E_F	O_E	***S***	***M***	***R***	E_F	O_E	***S***	***M***	***R***	E_F	O_E
1	80	19	1	0.1	0	75	23	2	0.1	0	70	20	10	0.3	3	78	14	8	0.4	3	82	13	5	0.3	1
5	77	20	4	0.2	1	70	18	13	0.4	5	67	12	20	0.6	13	66	21	14	0.4	6	75	19	6	0.2	1
10	79	14	7	0.3	2	71	10	18	0.6	12	63	7	30	0.8	24	68	13	19	0.6	11	82	12	6	0.3	2
24	67	21	12	0.4	4	59	13	28	0.7	19	56	2	42	1.0	40	57	13	30	0.7	21	77	15	7	0.3	2

[(a)] Conditions: source phase: 6 mL of 20 mM KPic; membrane: 6 mL of 0.625 mM carrier in $CHCl_3$; receiving phase: 6 mL of nanopure water.

Table 2

Mol percentages of sodium cations in the source (*S*), membrane (*M*) and receiving (*R*) phases at selected times during a period of 24 h at 303 K.[(a)] The efficiency factor (E_F) and overall efficiency (O_E) were calculated as described in the text.

t/h	Gi					mAGi					pAGi					DC18C6				
	S	***M***	***R***	E_F	O_E	***S***	***M***	***R***	E_F	O_E	***S***	***M***	***R***	E_F	O_E	***S***	***M***	***R***	E_F	O_E
1	73	24	3	0.1	0	81	12	7	0.4	3	67	28	6	0.2	1	87	8	5	0.4	2
5	69	20	12	0.4	5	60	19	21	0.5	11	66	10	23	0.7	16	71	11	18	0.6	11
10	66	15	19	0.6	11	60	2	38	1.0	36	60	4	36	0.9	32	66	1	33	1.0	32
24	59	9	31	0.8	24	54	5	42	0.9	38	49	8	43	0.8	36	52	7	42	0.9	36

[(a)] Conditions: source phase: 6 mL of 20 mM NaPic; membrane: 6 mL of 0.625 mM carrier in $CHCl_3$; receiving phase: 6 mL of nanopure water.

Supramol Chem. Author manuscript; available in PMC 2011 November 1.

Table 3

Mol percentages of lithium cations in the source (S), membrane (M) and receiving (R) phases at selected times during a period of 24 h at 303 K.[(a)] The efficiency factor (E_F) and overall efficiency (O_E) were calculated as described in the text.

t/h	Gi					mAGi					pAGi					DC18C6				
	S	***M***	***R***	E_F	O_E	***S***	***M***	***R***	E_F	O_E	***S***	***M***	***R***	E_F	O_E	***S***	***M***	***R***	E_F	O_E
1	79	16	5	0.2	1	90	8	2	0.2	0	94	1	5	0.8	4	85	5	10	0.7	7
5	75	17	8	0.3	3	90	5	5	0.5	3	76	16	8	0.3	3	76	12	12	0.5	6
10	77	13	10	0.4	4	87	3	10	0.8	8	85	6	9	0.6	5	75	14	11	0.4	5
24	69	11	20	0.6	13	88	4	8	0.7	5	78	14	7	0.3	2	78	13	10	0.4	4

[(a)] Conditions: source phase: 6 mL of 20 mM LiPic; membrane: 6 mL of 0.625 mM carrier in $CHCl_3$; receiving phase: 6 mL of nanopure water.

Table 4

Mol percentages of strontium cations in the source (*S*), membrane (*M*) and receiving (*R*) phases at selected times during a period of 24 h at 303 K.[(a)] The efficiency factor (E_F) and overall efficiency (O_E) were calculated as described in the text.

t/h	Gi					mAGi					pAGi					DC18C6				
	S	***M***	***R***	E_F	O_E	***S***	***M***	***R***	E_F	O_E	***S***	***M***	***R***	E_F	O_E	***S***	***M***	***R***	E_F	O_E
1	78	9	13	0.6	8	69	19	12	0.4	5	73	15	12	0.4	5	68	21	12	0.4	4
5	71	14	15	0.5	8	58	23	19	0.5	9	63	16	21	0.6	12	78	7	15	0.7	10
10	71	15	14	0.5	7	68	6	26	0.8	21	58	13	29	0.7	20	67	19	14	0.4	6
24	71	14	16	0.5	9	50	20	31	0.6	19	53	11	36	0.8	28	66	19	15	0.4	7

[(a)] Conditions: source phase: 6 mL of 20 mM $SrPic_2$; membrane: 6 mL of 0.625 mM carrier in $CHCl_3$; receiving phase: 6 mL of nanopure water.

Supramol Chem. Author manuscript; available in PMC 2011 November 1.